Targeted Therapy for *BRAF^{V600E}* Malignant Astrocytoma

Theodore P. Nicolaides[1], Huifang Li[2], David A. Solomon[2], Sujatmi Hariono[1], Rintaro Hashizume[1], Krister Barkovich[1], Suzanne J. Baker[3], Barbara S. Paugh[3], Chris Jones[4], Tim Forshew[5], Guy F. Hindley[5], J. Graeme Hodgson[6], Jung-Sik Kim[2], David H. Rowitch[1], William A. Weiss[1], Todd A. Waldman[2], and C. David James[1]

Abstract

Purpose: Malignant astrocytomas (MA) are aggressive central nervous system tumors with poor prognosis. Activating mutation of *BRAF* (*BRAF^{V600E}*) has been reported in a subset of these tumors, especially in children. We have investigated the incidence of *BRAF^{V600E}* in additional pediatric patient cohorts and examined the effects of BRAF blockade in preclinical models of *BRAF^{V600E}* and wild-type *BRAF* MA.

Experimental Design: *BRAF^{V600E}* mutation status was examined in two pediatric MA patient cohorts. For functional studies, *BRAF^{V600E}* MA cell lines were used to investigate the effects of *BRAF* shRNA knockdown *in vitro*, and to investigate BRAF pharmacologic inhibition *in vitro* and *in vivo*.

Results: *BRAF^{V600E}* mutations were identified in 11 and 10% of MAs from two distinct series of tumors (six of 58 cases total). BRAF was expressed in all MA cell lines examined, among which *BRAF^{V600E}* was identified in four instances. Using the BRAF^{V600E}-specific inhibitor PLX4720, pharmacologic blockade of BRAF revealed preferential antiproliferative activity against *BRAF^{V600E}* mutant cells *in vitro*, in contrast to the use of shRNA-mediated knockdown of *BRAF*, which inhibited cell growth of glioma cell lines regardless of *BRAF* mutation status. Using orthotopic MA xenografts, we show that PLX4720 treatment decreases tumor growth and increases overall survival in mice-bearing *BRAF^{V600E}* mutant xenografts, while being ineffective, and possibly tumor promoting, against xenografts with wild-type *BRAF*.

Conclusions: Our results indicate a 10% incidence of activating *BRAF^{V600E}* among pediatric MAs. With regard to implications for therapy, our results support evaluation of BRAF^{V600E}-specific inhibitors for treating BRAF^{V600E} MA patients. *Clin Cancer Res; 17(24); 7595–604. ©2011 AACR.*

Introduction

Malignant astrocytomas (MA) are aggressive brain tumors that affect people of all ages. Current treatments are inadequate, with median survival being 14 months in adults (1). A recently published study involving the use of radiation and temozolomide in treating 90 pediatric patients with MA revealed only 22% survival at 3 years (2). Although the genomics of adult grade IV MA (i.e., glioblastoma: GBM) have been researched extensively, and in some cases comprehensively (3, 4), pediatric studies have been more limited. For the most part, our current understanding of the genetic etiology of pediatric MAs is based on the examination of selected genes most commonly altered in corresponding adult tumors. The results of such studies indicate that the incidence of 2 of the most common gene alterations in adult MAs, epidermal growth factor receptor (*EGFR*) amplification and *PTEN* inactivation, are significantly reduced in pediatric MAs (5, 6). In contrast, other genetic alterations that have been linked with the pathogenesis of adult MA, such as those resulting in *TP53* and *CDKN2A* inactivation, occur at significant frequencies in pediatric MAs as well (7–9).

The receptor tyrosine kinase (RTK)-RAS-RAF-MEK-ERK signaling pathway relays extracellular signals from cell membrane-based RTKs to the nucleus via a series of consecutive phosphorylation events (10, 11). RTK-RAS-RAF-MEK-ERK signaling plays an important role in the pathogenesis of adult MAs (12), and increasing evidence

Authors' Affiliations: [1]University of California, San Francisco, San Francisco, California; [2]Georgetown University, Washington, District of Columbia; [3]St. Jude Children's Research Hospital, Memphis, Tennessee; [4]Institute of Cancer Research/Royal Marsden Hospital, Sutton; [5]Queen Mary University of London, London, United Kingdom; and [6]Pfizer, La Jolla, California

Note: Supplementary data for this article are available at Clinical Cancer Research Online (http://clincancerres.aacrjournals.org/).

T.P. Nicolaides and H. Li contributed equally to this work.

Corresponding Authors: Theodore Nicolaides, Department of Pediatrics, 505 Parnassus Ave., M649, University of California, San Francisco, San Francisco, CA 94143. Phone: 415-476-3831; E-mail: Theodore.nicolaides@ucsf.edu and C. David James, Department of Neurosurgery, Brain Tumor Research Center, 1450 3rd Street, Room HD283 Northwest, University of California, San Francisco, San Francisco, CA 94158. Phone: 415-476-5876; Fax: 415-502-0613; E-mail: david.james@ucsf.edu

Translational Relevance

Malignant astrocytoma (MA) is the most common histopathologic subclassification for primary central nervous system cancer, and the outcome for patients with MA is dismal. In the current study, we show a 10% incidence of BRAF^{V600E} in pediatric MAs, and show that a BRAF small molecule inhibitor has substantial activity against intracranial xenografts established from BRAF^{V600E} MA cells, while being ineffective against intracranial xenografts established from wild-type BRAF MA cells. This finding suggests that patients with BRAF^{V600E} MA can be effectively treated with BRAF-specific small molecule inhibitors. Because there is a clinically approved analog for the BRAF inhibitor we have used in our studies, we anticipate these results to have immediate impact with regard to stimulating clinical trial evaluation of BRAF small molecule inhibitors for treating patients with BRAF^{V600E} MA.

supports the importance of this pathway in the development of pediatric MAs as well (13–15). Activation of the RTK-RAS-RAF-MEK-ERK signaling in adult MA is usually associated with abnormal signaling of upstream RTKs, such as EGFR and platelet-derived growth factor receptor (PDGFR) (3). Inactivation of the *NF1* tumor suppressor gene, which encodes a RAS-GTPase, also leads to the activation of this pathway in adult MA (3, 16). Oncogenic mutation of other RTK-RAS-RAF-MEK-ERK signaling components, such as K-RAS, N-RAS, or BRAF, which commonly occur in a wide variety of human cancers, is infrequent in adult MA (17).

Recent publications suggest that RAF gene alterations occur at a higher frequency in pediatric astrocytomas, including pilocytic astrocytomas, pleomorphic xanthoastrocytomas, and MAs (13, 18). There are 3 RAF family proteins: A-, B-, and CRAF (RAF-1). In rodent brain, ARAF is rarely expressed, whereas both BRAF and CRAF are expressed in normal CNS tissue (19). ARAF has the lowest intrinsic kinase activity, followed by CRAF, with BRAF having highest intrinsic activity (20). All 3 RAF isoforms share RAS as a common activator, and MEK as a common substrate (21). With respect to the genes encoding these proteins, *BRAF* T1799A (*BRAF^{V600E}*) is the most common activating mutation, occurring in a broad spectrum of human tumors (22). BRAF^{V600E} is constitutively active, requires neither interaction with RAS nor dimer formation to signal, and is refractory to negative feedback inhibition (23). A recent report from our group describes activation of MAP kinase signaling in nearly all pediatric MAs, some of which have associated *BRAF^{V600E}* (13).

The discovery of activating *BRAF* mutation in pediatric MA's provides a unique opportunity to improve treatment outcomes for a subset of patients with this devastating disease. Small molecule kinase inhibitors that specifically target BRAF^{V600E} have recently been developed and show remarkable efficacy against melanomas that harbor this mutation (24). A recent phase I study using BRAF^{V600E}-specific inhibitor PLX4032 showed a response rate of 81% in a group of 48 patients with BRAF^{V600E}-positive metastatic melanoma (25).

In this study, we confirm the presence of *BRAF^{V600E}* mutation in 2 additional cohorts of pediatric MA. To investigate the importance of BRAF^{V600E} to MA growth, BRAF expression was suppressed in multiple MA cell lines by shRNA knockdown, with resultant determination that reduced levels of BRAF decreases ERK phosphorylation and results in decreased cell growth irrespective of tumor cell *BRAF^{V600E}* status. In contrast, a BRAF pharmacologic inhibitor shows BRAF^{V600E} dependency with regard to *in vitro* and *in vivo* MA antiproliferative effects.

Materials and Methods

Cell lines, xenografts, and primary tumors

MA cell lines were obtained from the American Type Culture Collection, DSMZ—the German Resource Centre for Biological Material, and the Japan Health Sciences Foundation Health Science Research Resources bank. Normal human astrocytes (NHA) were obtained from Clonetics and AllCells. All cell sources were authenticated through DNA fingerprinting using the Promega Powerplex platform.

Patient tissues from Royal Marsden Hospital, Sutton, and Newcastle Royal Infirmary, United Kingdom, were obtained after approval by Local and Multicenter Ethical Review Committees. Tumor DNAs were extracted from formalin fixed and paraffin-embedded (FFPE) tissues and whole genome amplified, as described previously (15). For the St. Jude tumors, sections from FFPE tissue were reviewed by 2 neuropathologists for identification of specimens suitable for DNA extraction from corresponding snap-frozen specimens, as previously described (26).

BRAF sequencing

The BRAF V600E hotspot region was amplified using primers BRAF_Ex_15_FFPE_F (TTCATGAAGACCTCACAG-TAAAAA) and BRAF_Ex_15_FFPE_R (CCACAAAATG-GATCCAGACA), which are designed to yield correct target sequence product by touchdown PCR. DNA was sequenced in both directions using the di-deoxy chain termination method on an ABI 3730 DNA Sequencer. Results were examined using the Applied Biosystems Sequence Scanner Software v1.0.

Western blot analysis

Cells and tissues were lysed in cell lysis buffer (Cell Signaling) supplemented with proteinase (Roche) and phosphatase (Sigma) inhibitor cocktails. Lysates were separated by SDS-PAGE and transferred to polyvinylidene difluoride membranes. After probing with primary antibodies, the membranes were incubated with

horseradish peroxidase-conjugated secondary antibody, and visualized by ECL (Pierce). Antibodies specific for total ERK, p-ERK, total MEK1/2, p-MEK1/2, total AKT, p-AKT-Ser473, CYCLIN D1, CYCLIN D3, CDK4 and CDK6, and p27[KIP1], were obtained from Cell Signaling Technologies. Antibody specific for BRAF was from Santa Cruz Biotechnology, CRAF from Upstate Biotechnology, and α-TUBULIN from Neomarkers.

Lentivirus mediated BRAF shRNA expression

Constructs for stable suppression of BRAF expression were obtained from The RNAi Consortium via Open Biosystems. A total of 12 constructs were obtained and tested to identify those able to achieve efficient BRAF protein knockdown. Negative control constructs in the same vector system (vector alone and scrambled shRNA) were obtained from Addgene. The lentiviral helper plasmids pHR′8.2ΔR and pCMV-VSV-G were also obtained from Addgene. The integrity of all plasmids was confirmed by restriction analysis, and the integrity of all shRNA inserts was confirmed by sequencing. Lentivirus preparation and infection of GBM cell lines have been described previously (27).

Cell growth assay

Stably infected GBM cells were plated into 96-well plates at a density of 100 to 500 cells/well and the medium was changed every 3 days. After selected incubation times, cell viabilities were determined with "CellTiter Glo Kit" from Promega and/or "Cell Counting Kit-8" from Dojindo Molecular Technologies. All cell growth analyses were conducted with 4 to 8 replicates.

Cell-cycle analysis

Cell-cycle distributions were determined by flow cytometric analysis following staining with propidium iodide. In brief, exponentially growing cells were harvested and fixed in 70% ethanol, then stained in PBS-buffered saline containing 0.1% Triton X-100, 50 μg/mL RNase, and 50 μg/mL propidium iodide, for 60 minutes at room temperature. The fluorescence was measured on a FACSort flow cytometer (Becton Dickinson), and data were analyzed using ModFit software (Verity Software House). Small molecule inhibitors used in association with cell-cycle analysis were PLX4720 (Plexxikon Inc.), Sorafenib, and GDC-0941, with the latter 2 obtained from Selleck Chemicals.

Modification of tumor cells with firefly luciferase reporter

Lentiviral vectors containing firefly luciferase (Fluc) were generated as previously described (28). AM-38 human MA cells were transduced with Fluc lentivirus as previously described for U87 cells (29). Cells were screened *in vitro* for transduction efficiency by treatment with luciferin (D-luciferin potassium salt, 150 mg/kg, Gold Biotechnology), and analysis for luminescence using a Xenogen IVIS Lumina System (Xenogen Corp.).

In vivo experiments

Five-week-old female athymic mice (nu/nu genotype, BALB/c background) were purchased from Simonsen Laboratories. Animals were housed under aseptic conditions. The UCSF Institutional Animal Care and Use Committee approved all animal protocols. Tumor cells were implanted into the brains of athymic mice as previously described (30). *In vivo* bioluminescence imaging (BLI) was carried out using the Xenogen IVIS Lumina System coupled to LivingImage data-acquisition software (Xenogen Corp.). Mice were anesthetized with 100 mg/kg of ketamine and 10 mg/kg of xylazine and imaged 10 minutes after intraperitoneal (i.p.) injection of luciferin. Signal intensity was quantified using LivingImage software.

To evaluate the therapeutic response of intracranial glioma xenografts, mice implanted with luciferase-modified MA cells were randomized to vehicle control [dimethyl sulfoxide (DMSO)] or PLX4720 treatment groups. Mice receiving PLX4720 treatments were administered a daily dose of 20 mg/kg by i.p. injection for 14 consecutive days. Treatment was initiated at day 7 postimplantation of tumor cells. All mice were monitored every day for the development of symptoms related to tumor burden, and 1 to 2× weekly by BLI. Mice were euthanized when they exhibited symptoms indicative of significant compromise to neurologic function. The Kaplan–Meier estimator was used to generate survival curves, and differences between survival curves were calculated using a log-rank test. In addition to the mice used for the survival analysis, 2 presymptomatic mice within each cohort were sacrificed 2 hours after their 7th treatment, with their brains resected and either placed in formalin and prepared for immunohistochemical analysis, or dissected from surrounding normal brain and snap frozen for immunoblot analysis. IHC was carried out as previously described (30), using Ki-67 antibody from Ventana Inc.

Results

BRAF[V600E] mutation in malignant astrocytomas

In follow-up to our previous finding of *BRAF*[V600E] mutation in pediatric MAs (13), *BRAF*[V600E] status was determined in 2 additional tumor cohorts. As shown in Table 1, *BRAF*[V600E] mutation was found in 3 of 28 tumors in the ICR cohort, and 3 of 30 tumors in the cohort from St. Jude. Interestingly, all *BRAF*[V600E] mutations in these series were identified in MAs of grade IV malignancy (i.e., GBM). Our previously published study (13) combined with results in the current report indicate a *BRAF*[V600E] mutation frequency of 14% (11 of 78) in grade III + grade IV pediatric MAs. As in our previously report (13), *BRAF*[V600E] mutations and *PDGFRA* amplifications were found as mutually exclusive in the additional cohorts being reported here (Supplementary Tables S1 and S2). For the combined 78 MA's in 3 series of pediatric tumors, 9 instances of *PDGFRA* amplification were determined (12%: Supplementary Tables S1–3).

Table 1. *BRAFV600E* and *PDGFRA* status of pediatric MAs

St. Jude's cohort (30 patients)	BRAF[V600E]	Wild-type BRAF	All
Diagnosis-AA	0	8	8
Diagnosis-GBM	3	19	22
Median age at diagnosis (mo)	165.2 (128–198)	111 (9–213)	117 (9–213)
PDGFRA amplification	0	4	4
Institute of Cancer Research cohort (28 patients)	**BRAF[V600E]**	**Wild-type BRAF**	**All**
Diagnosis-AA	0	6	6
Diagnosis-GBM	3	19	22
Median age at diagnosis (mo)	146 (79–240)	137 (5–272)	138 (5–272)
PDGFRA amplification	0	3	3

NOTE: Thirty patients from **St. Jude Children Research Hospital** and 28 patients from the **Institute of Cancer Research** were screened for the presence of *BRAF[V600E]* and *PDGFRA* amplifications. Diagnosis, median age at diagnosis (range indicated in parentheses), and *PDGFRA* amplification status are also shown. For individual patient data, refer to Supplementary Tables S1 and S2. Abbreviations: AA, anaplastic astrocytoma; GBM, glioblastoma.

To confirm sustainable tumor cell sources for *BRAF[V600E]*-associated investigation, we examined 20 MA cell lines, 15 of which had been previously analyzed for *BRAF[V600E]* (22), for mutant sequence (Supplementary Table S4). This analysis confirmed V600E mutation in cell lines DBTRG-05MG, AM-38, NMC-G1, and KG-1-C. Three of 4 cell line mutations are heterozygous for *BRAF[V600E]* (Supplementary Fig. S1), with *BRAF[V600E]* homozygosity evident in AM-38 cells. Previously published data (22) combined with our results indicate a 10% incidence (4 of 41) of *BRAF[V600E]* in MA cell lines.

BRAF copy number and expression in MA cell lines and pediatric tumors

We examined the extent of variation in BRAF protein expression among MA cell lines, and in relation to BRAF expression in NHA. Modest increases in BRAF protein were evident in 16 (80%) tumor cell lines relative to NHA (Fig. 1). Only 1 cell line, 42MGBA, expressed appreciably less BRAF than NHA. Analysis of normalized BRAF expression values indicates that *BRAF[V600E]* status is not a significant determinant of tumor BRAF expression (Supplementary Fig. S2A), nor of BRAF copy number (Supplementary Table S4), for MA cell lines. Examination of BRAF mRNA expression in pediatric MAs (UCSF tumor series: see Supplementary Table S3) also indicates a lack of association between *BRAF[V600E]* status and BRAF expression (Supplementary Fig. S2, panel B), as well as between *BRAF[V600E]* and *BRAF* copy number (Supplementary Table S3).

We also assessed CRAF, p-ERK, and p-MEK levels in the MA cell lines, with results showing more variability in CRAF
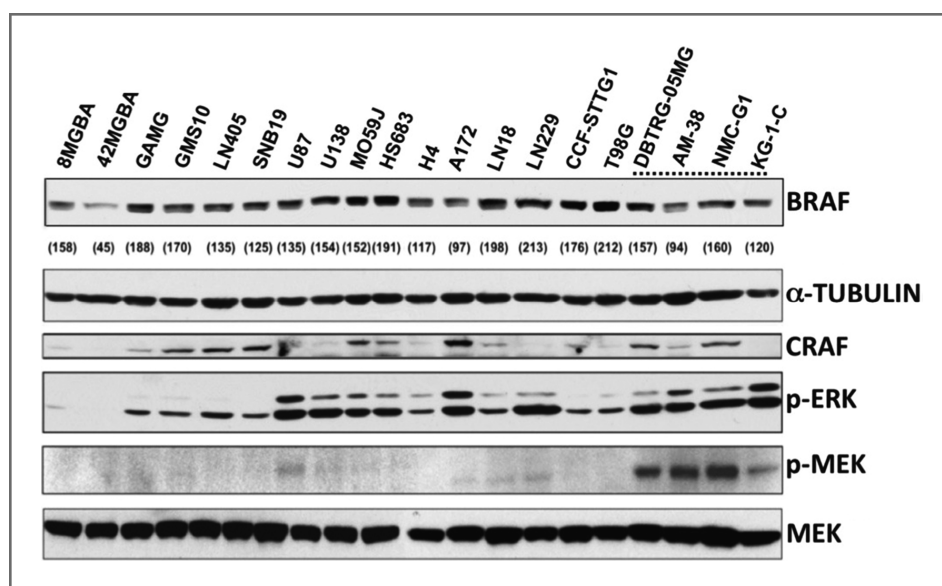

Figure 1. BRAF, CRAF, and downstream signaling mediator activation in MA cell lines. Cell lysates from 20 human MA cell lines were examined by Western blot using antibodies against the indicated proteins. Cell lines harboring mutant *BRAF* are indicated by the dotted line. BRAF protein signals were normalized against corresponding α-TUBULIN signals, with ratios expressed in relation to a NHA (Clonetics) value of 100. A second NHA cell source (AllCells) was determined as expressing nearly identical BRAF as the Clonetics NHAs that were used for establishing MA cell line BRAF expression levels.
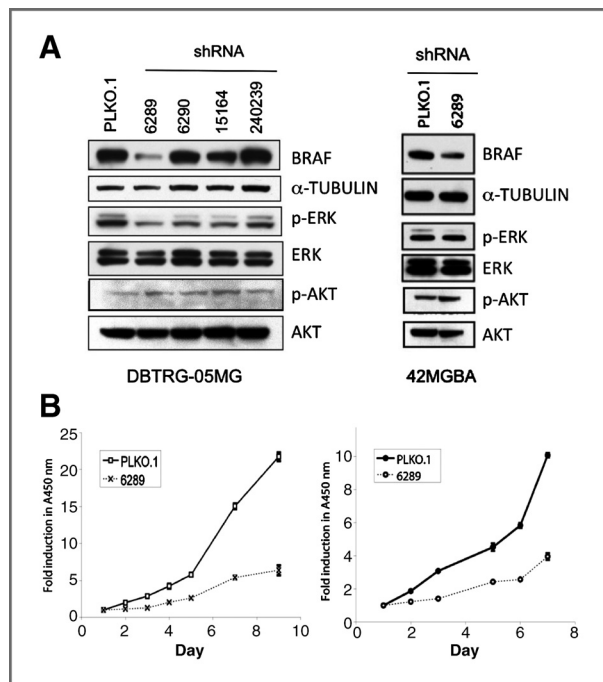
Figure 2. shRNA suppression of BRAF expression inhibits ERK phosphorylation and *in vitro* growth of MA cell lines. A, DBTRG-05MG cells were infected with lentivirus expressing empty vector (PLKO.1), or with each of 4 BRAF shRNA lentivirus. Results show that lentivirus 6289 is the most effective at suppressing BRAF expression, and being the most effective in suppressing phosphorylation of ERK. B, *in vitro* growth analysis of modified DBTRG-05MG cells (left) shows decreased growth rate of cells transduced with 6289 lentivirus. Control and 6289 shRNA derivatives for wild-type *BRAF* cell line 42MGBA were similarly examined for effects of BRAF knockdown on p-ERK (A, right) and cell proliferation (B, right).

expression than was evident for BRAF (Fig. 1). Phosphorylation of ERK was readily detectable in all of the MA cell lines except 2 (8MGBA and 42MGBA: Fig. 1). Inspection of the phospho-ERK levels indicates no apparent association with either BRAF expression level or *BRAF*^{V600E} status. In contrast, a clear association is indicated between *BRAF*^{V600E} status and phospho MEK levels (Fig. 1).

Inhibition of ERK phosphorylation and *in vitro* growth of MA cell lines by BRAF shRNA

Lentivirus expressing BRAF shRNA were screened for ability to suppress BRAF protein expression. Construct 6289 was the most effective in this regard (Fig. 2A), and was used to develop isogenic derivatives from 4 *BRAF*^{V600E} and 4 wild-type *BRAF* cell lines. Western blot results show that decreased BRAF protein is associated with suppression of ERK phosphorylation, as well as with inhibition of growth for all cell lines tested (Fig. 2A and B for representative results; additional results shown in Supplementary Fig. S3).

shRNA-mediated knockdown of BRAF results in G$_1$ phase arrest and altered expression of cell-cycle regulatory proteins

The antiproliferative effects of BRAF suppression were further investigated by comparison of cell-cycle distributions

for BRAF shRNA and control shRNA cells. In each of the 4 *BRAF*^{V600E} cell lines, BRAF knockdown increased G$_1$ phase fractions, primarily at the expense of cells in S phase (Fig. 3A). A lesser extent of G$_1$ increase from BRAF shRNA knockdown was evident in T98G cells, whereas shRNA knockdown resulted in little or no change in G$_1$ fraction for the 3 additional wild-type BRAF cell lines. Although initial inspection of the cell-cycle distributions could be interpreted as indicating that BRAF shRNA knockdown has little effect on the sub-G$_1$ fraction of all MA cell lines, substantially higher sub-G$_1$ increases were, in fact, evident in 2 of the 4 V600E cell lines (Supplementary Fig. S4).

The RTK-RAS-RAF-MEK-ERK signaling pathway activates several key cell-cycle regulatory proteins to promote G$_1$ to S transition (10). In particular, ERK activation has been shown to induce cell proliferation by increasing CYCLIN D1 and decreasing p27^{KIP1} levels in various cell types (31–34). Western blot results for the 4 *BRAF*^{V600E} cell lines showed that BRAF knockdown increased p27^{KIP1} or decreased CYCLIN D1, or both (Fig. 3B). For the MA cell lines with wild-type *BRAF*, shRNA suppression resulted in decreased CYCLIN D1 and increased p27^{KIP1} in 42MGBA and LN229, respectively. Investigation of additional cell-cycle regulatory proteins revealed that BRAF knockdown significantly decreased CYCLIN D3 protein in all MA cell lines except DBTRG-05MG (Fig. 3B). Protein levels of CDK4 or CDK6, or both, were also reduced by BRAF shRNA in all of the cell lines.

PLX4720 suppresses MEK-ERK phosphorylation and cell proliferation in MA cells containing *BRAF*^{V600E} mutation

As a complementary approach to investigating the suppression of BRAF expression in MA cells, we examined antiproliferative effects of the small molecule inhibitor PLX4720, a tool compound that is closely related to the PLX4032 inhibitor currently being evaluated in clinical trials against melanoma harboring *BRAF*^{V600E} (25). Dose–response curves for AM-38 and DBTRG05-MG (both *BRAF*^{V600E}), and 42MGBA (wild-type *BRAF*) show that PLX4720 inhibits cell growth irrespective of cell line V600E status (Fig. 4A), but that the 2 lines with *BRAF*^{V600E} are sensitive to much lower concentrations of the inhibitor: the EC$_{50}$ for DBTRG-05MG and AM-38 is 1.75 and 6.19 µmol/L, respectively, whereas the EC$_{50}$ of 42MGBA is 31.20 µmol/L. Corresponding Western blot results (Fig. 4B) show that PLX4720 inhibits phosphorylation of MEK and ERK in a dose dependent as well as a *BRAF*^{V600E}-dependent manner. In DBTRG-05MG and AM-38 cells, 2 µmol/L PLX4720 decreased EGF-induced MEK and ERK phosphorylation, whereas 50 µmol/L PLX4720 was needed to inhibit EGF-induced MEK/ERK phosphorylation in 42MGBA cells. Importantly, the lowest dose of PLX4720 (2 µmol/L) led to an activation of MEK/ERK signaling in 42MGBA, likely secondary to paradoxical activation of wild-type BRAF, as previously described (35–37).

Analysis of cell-cycle distribution effects of 2 µmol/L PLX4720 treatment revealed increased G$_1$ fraction and reduced S phase component in *BRAF*^{V600E} cells (Fig. 4C),
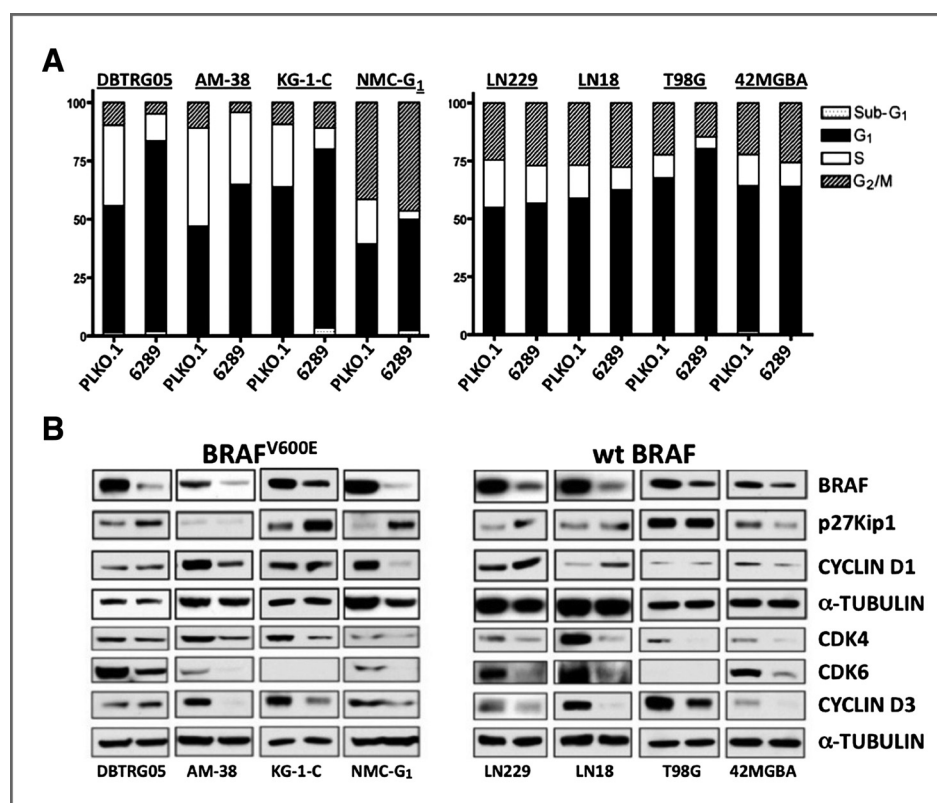
Figure 3. Effect of shRNA-mediated BRAF suppression on MA cell-cycle distributions and expression of cell-cycle regulatory proteins. A, MA cell lines with (left) or without (right) $BRAF^{V600E}$ mutation were infected with lentivirus expressing empty control (PLKO.1) or BRAF shRNA (6289), then treated with puromycin to select infected cells. Pooled puromycin-resistant cells were subjected to flow cytometry to determine cell-cycle distributions. For all cell lines with $BRAF^{V600E}$, suppression of BRAF expression resulted in increased proportion of G_1 phase cells. For 3 of 4 cell lines with wild-type $BRAF$, shRNA suppression had little effect on the G_1 fraction of cells. B, lysates from the same transduced cells as in A were subjected to Western blot analysis to assess the effects of BRAF knockdown on the expression of proteins with known roles in regulating G_1 phase cell-cycle transit: CYCLIN D1 and CYCLIN D3, enzymatic subunits CDK4 and CDK6, and cyclin-dependent kinase inhibitor $p27^{Kip1}$. The left lane in each blot results from control shRNA and the right lane result is from use of the BRAF shRNA lentivirus. Comparison of results for any 2 cell lines shows that BRAF suppression effects are variable for the 5 G_1 regulatory proteins examined, but are consistent in showing that BRAF suppression results in decreased expression of 1 or more of the proteins that promote G_1 transit, and/or increases the expression of the negative G_1 transit regulator $p27^{Kip1}$.
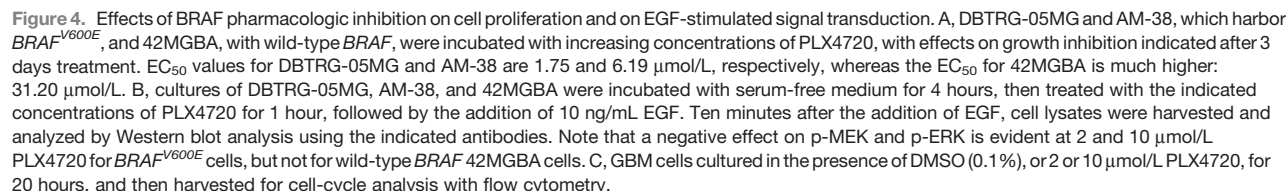
with the opposite response observed in wild-type BRAF cells: that is, decreased G_1 and increased S phase cell components for 42MGBA. At 10 µmol/L PLX4720 treatment, the G_1 and S phase responses of 42MGBA were reversed relative to 2 µmol/L responses, and despite indication of residual p-MEK/p-ERK (Fig. 4B). This reversal in effect is potentially associated with inhibitor off-target effects, as suggested by decreases in 42MGBA p-AKT at 10 and 50 µmol/L PLX4720 treatments (Fig. 4B).

Because 42MGBA has reduced expression of BRAF compared with NHA one might predict these cells to be less representative of wild-type BRAF MA cell response to BRAF inhibition. To address whether the lack of effect of PLX4720 on wild-type BRAF glioma cells was unique to 42MGBA, a second wild-type $BRAF$ cell line, U87, was also tested for PLX4720, with similar results obtained as for 42MGBA: that is, low dose PLX4720 treatment results in paradoxical activation of p-MEK and p-ERK, with corresponding decreases and increases in U87 G_1 and S phase components, respectively (Supplementary Fig. S5). Importantly, PLX4720

signaling pathway response for both wild-type BRAF (U87) and $BRAF^{V600E}$ (AM-38) cells were reproducible in serum-supplemented media (Supplementary Fig. S6).

Interestingly, 2 and 10 µmol/L PLX4720 resulted in little change to the sub-G_1 component of treated $BRAF^{V600E}$ cells (Fig. 4C). To address whether this lack of response was due to alternative signaling pathway protection from apoptosis, we examined the effect of concurrent BRAF + PI3K/mTOR inhibition. As shown in Supplementary Fig. S7, combined PI3K/mTOR and BRAF blockade leads to a further increase in G_1 arrest, but no significant increase in sub-G_1 component. This result suggests that MA cells primarily depend on the PI3K/mTOR and BRAF pathways for proliferation.

To address whether observed cell line responses to RAF inhibition were specific to treatment with PLX4720, we additionally tested wild-type $BRAF$ and $BRAF^{V600E}$ cells with sorafenib, a pan-RAF inhibitor. As shown in Supplementary Fig. S8, whereas sorafenib induces a dose-dependent decrease in p-MEK and p-ERK in both AM-38 and U87 cells, these signaling pathway changes occur without

Figure 4. Effects of BRAF pharmacologic inhibition on cell proliferation and on EGF-stimulated signal transduction. A, DBTRG-05MG and AM-38, which harbor *BRAF*^{V600E}, and 42MGBA, with wild-type *BRAF*, were incubated with increasing concentrations of PLX4720, with effects on growth inhibition indicated after 3 days treatment. EC$_{50}$ values for DBTRG-05MG and AM-38 are 1.75 and 6.19 μmol/L, respectively, whereas the EC$_{50}$ for 42MGBA is much higher: 31.20 μmol/L. B, cultures of DBTRG-05MG, AM-38, and 42MGBA were incubated with serum-free medium for 4 hours, then treated with the indicated concentrations of PLX4720 for 1 hour, followed by the addition of 10 ng/mL EGF. Ten minutes after the addition of EGF, cell lysates were harvested and analyzed by Western blot analysis using the indicated antibodies. Note that a negative effect on p-MEK and p-ERK is evident at 2 and 10 μmol/L PLX4720 for *BRAF*^{V600E} cells, but not for wild-type *BRAF* 42MGBA cells. C, GBM cells cultured in the presence of DMSO (0.1%), or 2 or 10 μmol/L PLX4720, for 20 hours, and then harvested for cell-cycle analysis with flow cytometry.

substantial change to the cell-cycle distributions of either type of cell. Thus, the antiproliferative effect of BRAF inhibition is specific to the use of the BRAF^{V600E} selective-inhibitor PLX4720 against *BRAF*^{V600E} cell lines.

PLX4720 represses growth of intracranial *BRAF*^{V600E} MA xenografts

To investigate the effects of BRAF pharmacologic inhibition *in vivo*, we utilized an orthotopic xenograft model approach, in which tumor cells, modified with a luciferase reporter, are monitored for response to treatment, following intracranial injection in athymic mice. Mice with intracranial AM-38 showed reduced intracranial tumor growth from PLX4720 treatment, relative to corresponding vehicle-treated mice, resulting in significantly prolonged survival (Fig. 5A). The survival of mice with intracranial DBTRG-05MG was also significantly extended from treatment with PLX4720 (data not shown). AM-38 tumors in mouse brain,

following 1 week of PLX4720 treatment, showed decreased Ki-67 staining, relative to tumor from a vehicle-treated mouse (Supplementary Fig. S9A and B), corroborating the *in vivo* antiproliferative treatment effect indicated by BLI. Western blot analysis of protein extract from AM-38 intracranial xenografts revealed that PLX4720 therapy decreases p-ERK (Supplementary Fig. S9C), consistent with *in vitro* results (Fig. 4).

To determine whether PLX4720 shows activity against wild-type *BRAF* xenografts, we established intracranial tumors with U87 cells that had been previously modified with luciferase lentivirus and used for investigation of response to cdk4/6 inhibition (29). PLX4720-treated mice bearing wild-type *BRAF* U87 xenografts showed no delayed tumor growth or survival advantage, consistent with *in vitro* results of U87 which indicated low sensitivity to PLX4720 (U87 EC$_{50}$ of 48.8 μmol/L, data not shown). In fact, results from bioluminescence monitoring
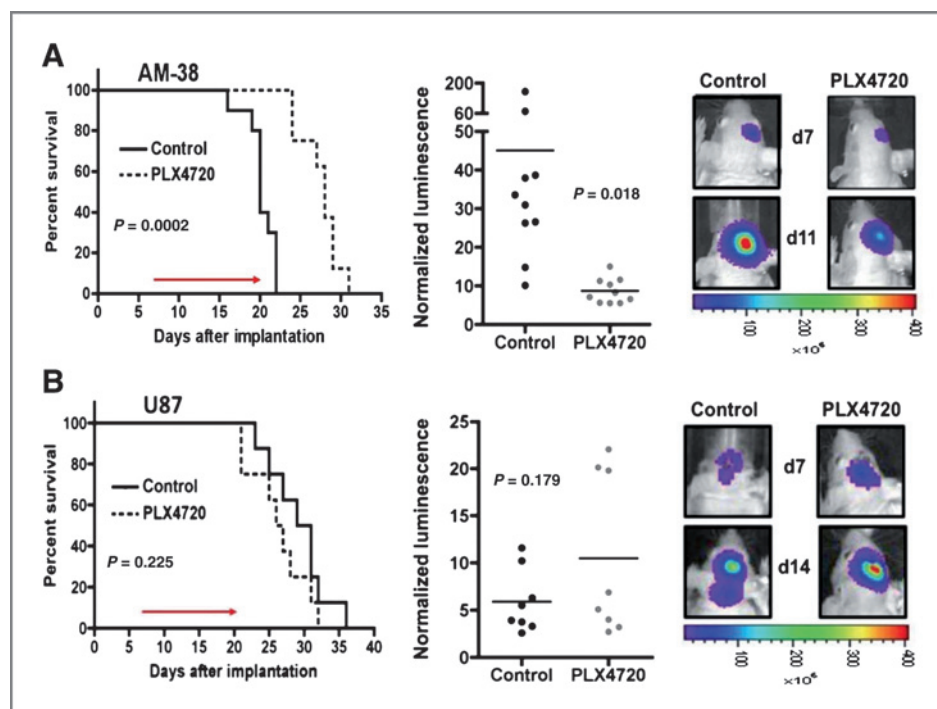
Figure 5. Effect of PLX4720 on tumor growth and survival for mice with intracranial MA xenografts. A, mice received intracranial injection of 300,000 luciferase modified *BRAF*^{V600E} AM-38 cells, with i.p. administration of vehicle (DMSO) or PLX4720 (20 mg/kg) daily for 2 weeks, beginning at day 7. Survival plot (left) shows that PLX4720 treatment significantly extends the survival of mice with intracranial *BRAF*^{V600E} tumors, consistent with results from quantitative BLI which show significant antiproliferative effect of PLX4720 at the first imaging time point subsequent to initiation of treatment ($P = 0.018$ for control vs. PLX4720 BLI values, middle). Bioluminescence images (right) of intracranial tumor in control and PLX4720 treatment group mice show lesser AM-38 bioluminescence signal in the mouse administered PLX4720 following the 5th day of PLX4720 treatment (mice shown had median treatment group luminescence values at time of initiation of therapy). B, in contrast, no PLX4720 survival advantage or antiproliferative effect is evident for mice with wild-type *BRAF* intracranial xenografts (U87).

indicated increased mean U87 xenograft growth rate and reduced survival from PLX4720 treatment (Fig. 5B). Results from Ki-67 staining of PLX4720-treated U87 tumors showed consistency with BLI results: Ki-67–positive cells were more abundant in PLX4720-treated tumor (Supplementary Fig. S9D and E).

Discussion

Patients with MAs have a poor prognosis. Despite aggressive therapy, relapse rates are high, with median survival being 14 months in adults (1), and the majority of pediatric MA patients succumbing to cancer within 3 years of diagnosis (2). There is a relative dearth of information regarding recurrent molecular characteristics in pediatric MAs that can be used for therapeutic hypothesis testing. *PDGFRA* amplification, though noted in a fraction of these tumors (13, 14, 38), has yet to be successfully exploited for improved MA patient outcomes from the use of PDGF receptor inhibitors (39). This is also the case for *EGFR* amplification in adult MAs, for which the use of EGFR small molecule inhibitors has yet to confer a clear survival benefit (40, 41). The lack of success in targeting EGF and PDGF receptors in treating brain tumor patients is perhaps a result of RTK functional redundancy that compensates for the blockade

of just 1 RTK (42). In principle, pathway blockade downstream of RTKs may be more successful, because numerous RTKs converge on a few key signaling nodes in promoting cell proliferation. In this study, we found that BRAF may represent such a point of signal convergence, because the growth of all tested MA cell lines was inhibited by suppression of BRAF expression (Fig. 2).

Although gain of function mutation of *KRAS*, *NRAS*, and *BRAF* are among the most frequently occurring oncogene alterations in cancer, such mutations are uncommon in adult MAs (17, 18). In spite of the low mutation incidence, RTK-RAS-RAF-MEK-ERK signaling is upregulated in most of these tumors, and high ERK activation correlates with poor prognosis for MA patients (43). In this study, we confirm the finding of *BRAF* activating mutations (*BRAF*^{V600E}) in a subset of pediatric MAs. BRAF^{V600E} was identified in 6 of 58 (10%) pediatric MAs, from 2 distinct series of tumors, and in 4 MA cell lines. *In vitro*, BRAF^{V600E} mutation was associated with elevated p-MEK levels. Because *BRAF* is located on chromosome 7 (q35), and gain of chromosome 7 is frequently detected in MAs, *BRAF* copy number is commonly increased in these tumors (44). We also found copy number gains of *BRAF* in most MA cell lines and primary tumors, although no focal or high-level *BRAF* amplifications were evident (Supplementary Tables S3and

S4). In addition to *BRAF* copy number increases and mutation, we found elevated expression of BRAF protein, relative to NHA, in a majority of MA cell lines (Fig. 1).

Our results show that inhibition of BRAF expression by shRNA knockdown leads to decreased p-ERK levels and reduced proliferation of MA cell lines, independent of *BRAF*^{V600E} status (Fig. 2; Supplementary Fig. S3). However, inspection of flow cytometry results from BRAF shRNA-modified cells (Fig. 3A), for cell-cycle effects of BRAF shRNA, reveals a more rapid antiproliferative effect of BRAF knockdown on BRAF^{V600E} cells, suggesting increased cellular proliferation dependence on, and addiction to BRAF signaling for BRAF^{V600E} cells. This dependence is further indicated by results from BRAF pharmacologic inhibition with PLX4720, which show specificity of antiproliferative effect for tumor cell lines and xenografts with V600E (Figs. 4 and 5). PLX4720 BRAF blockade resulted in MAPK pathway inhibition, decreased growth rate, and increased G_1 arrest in cell lines with *BRAF*^{V600E}, whereas *BRAF* wild-type cells, when treated with low doses of PLX4720, show increased MAPK activation and a decrease in G_1 phase cells. Observation of a stimulatory effect of BRAF inhibition on MAPK activation in cells with wild-type BRAF has been reported by others (35–37). It is important to note that BRAF^{V600E} inhibition did not promote substantial apoptotic response of BRAF-mutant cells, and that combined BRAF + PI3K/mTOR blockade led only to further G_1 arrest, without increased sub-G_1 component (Supplementary Fig. S7). These data suggest that MA cells primarily depend on the PI3K/mTOR and BRAF pathways for proliferation, and not so much for survival.

To extend *in vitro* observations to the *in vivo* setting, we generated intracranial xenografts using MA cell lines with and without *BRAF*^{V600E}. Our results (Fig. 5) show that BRAF inhibition by PLX4720 significantly decreases tumor growth rate (as indicated by quantitative BLI), with corresponding increase in survival for mice carrying *BRAF*-mutant xenografts, and to an extent showing reasonable consistency with length of treatment. Experiments are ongoing to determine maximal extent of PLX4720 survival benefit, given sustained daily treatment, and using multiple MA

models. Molecular analysis of PLX4720-treated *BRAF*^{V600E} tumors shows decreased p-ERK *in vivo* (Supplementary Fig. S9C) and decreased Ki-67 staining (Supplementary Fig. S9A and B). These results are consistent with the decreased tumor cell proliferation indicated by BLI monitoring. In contrast, U87 xenografts, harboring wild-type *BRAF*, did not respond to PLX4720, and, in fact, showed a trend toward increased tumor growth rate and decreased survival (Fig. 5B, Supplementary Fig. S9D and E).

BRAF^{V600E} is now a validated therapeutic target in metastatic melanoma, with high response rates reported using both the Plexxikon BRAF^{V600E}–specific inhibitor PLX4032 (25) and the Glaxo Smith Kline inhibitor GSK2118436 (45). Phase III studies suggest a survival advantage for patients treated with PLX4032, when compared with standard chemotherapy (46). Taken together with the results reported here, there is a highly supportive rationale for using BRAF-specific pharmacologic inhibition in treating MAs with *BRAF*^{V600E}.

Disclosure of Potential Conflicts of Interest

No potential conflicts of interest were disclosed.

References

1. Stupp R, Mason WP, van den Bent MJ, Weller M, Fisher B, Taphoorn MJ, et al. Radiotherapy plus concomitant and adjuvant temozolomide for glioblastoma. N Engl J Med 2005;352:987–96.
2. Cohen KJ, Heideman RL, Zhou T, Holmes EJ, Lavey RS, Bouffet E, et al. Temozolomide in the treatment of children with newly diagnosed diffuse intrinsic pontine gliomas: a report from the Children's Oncology Group. Neuro Oncol 2011;13:410–6.
3. Cancer Genome Atlas Research Network. Comprehensive genomic characterization defines human glioblastoma genes and core pathways. Nature 2008;455:1061–8.
4. Parsons DW, Jones S, Zhang X, Lin JC, Leary RJ, Angenendt P, et al. An integrated genomic analysis of human glioblastoma multiforme. Science 2008;321:1807–12.
5. Pollack IF, Hamilton RL, James CD, Finkelstein SD, Burnham J, Yates AJ, et al. Rarity of PTEN deletions and EGFR amplification in malignant gliomas of childhood: Results from the children's cancer group 945 cohort. J Neurosurg 2006;105:418–24.
6. Ganigi PM, Santosh V, Anandh B, Chandramouli BA, Sastry Kolluri VR. Expression of p53, EGFR, pRb and bcl-2 proteins in pediatric glioblastoma multiforme: A study of 54 patients. Pediatr Neurosurg 2005;41:292–9.
7. Pollack IF, Finkelstein SD, Burnham J, Hamilton RL, Yates AJ, Holmes EJ, et al. Age and TP53 mutation frequency in childhood malignant gliomas: Results in a multi-institutional cohort. Cancer Res 2005;61:7404–7.
8. Pollack IF, Finkelstein SD, Woods J, Burnham J, Holmes EJ, Hamilton RL, et al. Expression of p53 and prognosis in children with malignant gliomas. N Engl J Med 2003;346:420–7.
9. Sure U, Ruedi D, Tachibana O, Yonekawa Y, Ohgaki H, Kleihues P, et al. Determination of p53 mutations, EGFR overexpression, and loss of p16 expression in pediatric glioblastomas. J Neuropathol Exp Neurol 1997;56:782–9.
10. Sebolt-Leopold JS, Herrera R. Targeting the mitogen-activated protein kinase cascade to treat cancer. Nat Rev Cancer 2004;4:937–47.
11. McKay MM, Morrison DK. Integrating signals from RTKs to ERK/MAPK. Oncogene 2007;26:3113–21.

12. Lopez-Gines C, Gil-Benso R, Benito R, Mata M, Pereda J, Sastre J, Roldan P, et al. The activation of ERK1/2 MAP kinases in glioblastoma pathobiology and its relationship with EGFR amplification. Neuropathol 2008;28:507–15.

13. Schiffman JD, Hodgson JG, VandenBerg SR, Flaherty P, Polley MY, Yu M, et al. Oncogenic BRAF mutation with CDKN2A inactivation is characteristic of a subset of pediatric malignant astrocytomas. Cancer Res 2010;70:512–9.

14. Paugh BS, Qu C, Jones C, Liu Z, Adamowicz-Brice M, Zhang J, et al. Integrated molecular genetic profiling of pediatric high-grade gliomas reveals key differences with the adult disease. J Clin Oncol 2010; 28:3061–8.

15. Bax DA, Mackay A, Little SE, Carvalho D, Viana-Pereira M, Tamber N, et al. A distinct spectrum of copy number aberrations in pediatric high-grade gliomas. Clin Cancer Res 2010;16:3368–77.

16. McGillicuddy LT, Fromm JA, Hollstein PE, Kubek S, Beroukhim R, De Raedt T, et al. Proteasomal and genetic inactivation of the NF1 tumor suppressor in gliomagenesis. Cancer Cell 2009;16:44–54.

17. Knobbe CB, Reifenberg J, Reifenberger G. Mutation analysis of the ras pathway genes NRAS, HRAS, KRAS and BRAF in glioblastomas. Acta Neuropathol 2004;108:467–70.

18. Schindler G, Capper D, Meyer J, Janzarik W, Omran H, Herold-Mende C, et al. Analysis of BRAF V600E mutation in 1,320 nervous system tumors reveals high mutation frequencies in pleomorphic xanthoastrocytoma, ganglioglioma and extra-cerebellar pilocytic astrocytoma. Acta Neuropathol 2011;121:397–405.

19. Morice C, Nothias F, Konig S, Vernier P, Baccarini M, Vincent JD, et al. RAF-1 and BRAF proteins have similar regional distributions but differential subcellular localization in adult rat brain. Eur J Neurosci 1999;11:1995–2006.

20. Wellbrock C, Karasarides M, Marais R. The RAF proteins take centre stage. Nat Rev Mol Cell Biol 2004;5:875–85.

21. Marais R, Light Y, Paterson HF, Mason CS, Marshall CJ. Differential regulation of raf-1, A-raf, and BRAF by oncogenic ras and tyrosine kinases. J Biol Chem 1997;272:4378–83.

22. Davies H, Bignell GR, Cox C, Stephens P, Edkins S, Clegg S, et al. Mutations of the BRAF gene in human cancer. Nature 2002;417: 949–54.

23. Tsavachidou D, Coleman ML, Athanasiadis G, Li S, Licht JD, Olson MF, et al. SPRY2 is an inhibitor of the ras/extracellular signal-regulated kinase pathway in melanocytes and melanoma cells with wild-type BRAF but not with the V599E mutant. Cancer Res 2004; 64:5556–9.

24. Tsai J, Lee JT, Wang W, Zhang J, Cho H, Mamo S, et al. Discovery of a selective inhibitor of oncogenic BRAF kinase with potent antimelanoma activity. Proc Natl Acad Sci U S A 2008;105: 3041–6.

25. Flaherty KT, Puzanov I, Kim KB, Ribas A, McArthur GA, Sosman JA, et al. Inhibition of mutated, activated BRAF in metastatic melanoma. N Engl J Med 2010;363:809–19.

26. Torchia EC, Boyd K, Rehg JE, Qu C, Baker SJ. EWS/FLI-1 induces rapid onset of myeloid/erythroid leukemia in mice. Mol Cell Biol 2007;27:7918–34.

27. Kim JS, Lee C, Bonifant CL, Ressom H, Waldman T. Activation of p53-dependent growth suppression in human cells by mutations in PTEN or PIK3CA. Mol Cell Biol 2007;27:662–77.

28. Sarkaria JN, Yang L, Grogan PT, Kitange GJ, Carlson BL, Schroeder MA, et al. Identification of molecular characteristics correlated with glioblastoma sensitivity to EGFR kinase inhibition through use of an intracranial xenograft test panel. Mol Cancer Ther 2007;6: 1167–74.

29. Michaud K, Solomon DA, Oermann E, Kim JS, Zhong WZ, Prados MD, et al. Pharmacologic inhibition of cyclin-dependent kinases 4 and 6 arrests the growth of glioblastoma multiforme intracranial xenografts. Cancer Res 2010;70:3228–38.

30. Hashizume R, Gupta N, Berger MS, Banerjee A, Prados MD, Ayers-Ringler J, et al. Morphologic and molecular characterization of ATRT

xenografts adapted for orthotopic therapeutic testing. Neuro Oncol 2010;12:366–76.

31. Bhatt KV, Hu R, Spofford LS, Aplin AE. Mutant BRAF signaling and cyclin D1 regulate Cks1/S-phase kinase-associated protein 2-mediated degradation of p27Kip1 in human melanoma cells. Oncogene 2007;26:1056–66.

32. Schiappacassi M, Lovat F, Canzonieri V, Belletti B, Berton S, Di Stefano D, et al. p27Kip1 expression inhibits glioblastoma growth, invasion, and tumor-induced neoangiogenesis. Mol Cancer Ther 2008;7:1164–75.

33. Lavoie JN, L'Allemain G, Brunet A, Müller R, Pouysségur J. Cyclin D1 expression is regulated positively by the p42/p44MAPK and negatively by the p38/HOGMAPK pathway. J Biol Chem 1996; 271:20608–16.

34. Gysin S, Lee SH, Dean NM, McMahon M. Pharmacologic inhibition of RAF–>MEK–>ERK signaling elicits pancreatic cancer cell cycle arrest through induced expression of p27Kip1. Cancer Res 2005;65:4870–80.

35. Poulikakos PI, Zhang C, Bollag G, Shokat KM, Rosen N. RAF inhibitors transactivate RAF dimers and ERK signalling in cells with wild-type BRAF. Nature 2010;464:427–30.

36. Hatzivassiliou G, Song K, Yen I, Brandhuber BJ, Anderson DJ, Alvarado R, et al. RAF inhibitors prime wild-type RAF to activate the MAPK pathway and enhance growth. Nature 2010;464:431–5.

37. Heidorn SJ, Milagre C, Whittaker S, Nourry A, Niculescu-Duvas I, Dhomen N, et al. Kinase-dead BRAF and oncogenic RAS cooperate to drive tumor progression through CRAF. Cell 2010;140: 209–21.

38. Zarghooni M, Bartels U, Lee E, Buczkowicz P, Morrison A, Huang A, et al. Whole-genome profiling of pediatric diffuse intrinsic pontine gliomas highlights platelet-derived growth factor receptor alpha and poly (ADP-ribose) polymerase as potential therapeutic targets. J Clin Oncol 2010;28:1337–44.

39. Pollack IF, Jakacki RI, Blaney SM, Hancock ML, Kieran MW, Phillips P, et al. Phase I trial of imatinib in children with newly diagnosed brainstem and recurrent malignant gliomas: A pediatric brain tumor consortium report. Neuro Oncol 2007;9:145–60.

40. Prados MD, Chang SM, Butowski N, DeBoer R, Parvataneni R, Carliner H, et al. Phase II study of erlotinib plus temozolomide during and after radiation therapy in patients with newly diagnosed glioblastoma multiforme or gliosarcoma. J Clin Oncol 2009;27:579–84.

41. Brown PD, Krishnan S, Sarkaria JN, Wu W, Jaeckle KA, Uhm JH, et al. Phase I/II trial of erlotinib and temozolomide with radiation therapy in the treatment of newly diagnosed glioblastoma multiforme: North central cancer treatment group study N0177. J Clin Oncol 2008; 26:5603–9.

42. Stommel JM, Kimmelman AC, Ying H, Nabioullin R, Ponugoti AH, Wiedemeyer R, et al. Coactivation of receptor tyrosine kinases affects the response of tumor cells to targeted therapies. Science 2007; 318:287–90.

43. Mawrin C, Diete S, Treuheit T, Kropf S, Vorwerk CK, Boltze C, et al. Prognostic relevance of MAPK expression in glioblastoma multiforme. Int J Oncol 2003;23:641–8.

44. Jeuken J, van den Broecke C, Gijsen S, Boots-Sprenger S, Wesseling P. RAS/RAF pathway activation in gliomas: The result of copy number gains rather than activating mutations. Acta Neuropathol 2007; 114:121–33.

45. Long GV, Kefford RF, Carr PJA, et al. Phase 1/2 study of Gsk2118436, a selective inhibitor of V600 mutant (Mut) Braf Kinase: evidence of activity in melanoma brain metastases (Mets). European Society of Medical Oncolgy Congress 2010. Late Breaking Abstract. Ann Oncol 2010;21(Suppl 8): NP doi:10.1093/annonc/mdq601. Abstract LBA27.

46. Chapman PB, Hauschild A, Robert C, Haanen JB, Ascierto P, Larkin J, et al. BRIM-3 Study Group. Improved survival with vemurafenib in melanoma with BRAF V600E mutation. N Engl J Med 2011; 364:2507–16.

AACR American Association
for Cancer Research

Clinical Cancer Research

Targeted Therapy for *BRAF*^{V600E} Malignant Astrocytoma

Theodore P. Nicolaides, Huifang Li, David A. Solomon, et al.

Updated version	Access the most recent version of this article at: doi:10.1158/1078-0432.CCR-11-1456
Supplementary Material	Access the most recent supplemental material at: http://clincancerres.aacrjournals.org/content/suppl/2011/10/27/1078-0432.CCR-11-1456.DC2.html

Cited articles	This article cites 45 articles, 21 of which you can access for free at: http://clincancerres.aacrjournals.org/content/17/24/7595.full.html#ref-list-1
Citing articles	This article has been cited by 19 HighWire-hosted articles. Access the articles at: http://clincancerres.aacrjournals.org/content/17/24/7595.full.html#related-urls

E-mail alerts	Sign up to receive free email-alerts related to this article or journal.
Reprints and Subscriptions	To order reprints of this article or to subscribe to the journal, contact the AACR Publications Department at pubs@aacr.org.
Permissions	To request permission to re-use all or part of this article, contact the AACR Publications Department at permissions@aacr.org.